Swenson, R. P., & Howard, J. B. (1979) *J. Biol. Chem. 254*, 4452–4456.
Swenson, R. P., & Howard, J. B. (1980) *J. Biol. Chem. 255*, 8087–8091.
Vanaman, T. C., & Stark, G. R. (1970) *J. Biol. Chem. 245*, 3565–3573.
Van Leuven, F., Cassiman, J. J., & Van den Berghe, H. (1981) *J. Biol. Chem. 256*, 9016–9022.
Van Leuven, F., Marynen, P., Cassiman, J. J., & Van den Berghe, H. (1982a) *Biochem. J. 203*, 405–411.
Van Leuven, F., Cassiman, J. J., & Van der Berghe, H. (1982b) *Biochem. J. 201*, 119–128.

Metal Ion Dependence of Phosphorothioate ATP Analogues in the *Bacillus stearothermophilus* Tyrosyl-tRNA Synthetase Reaction†

George A. Garcia,‖ Robin J. Leatherbarrow,‡ Fritz Eckstein,§ and Alan R. Fersht*
MRC Unit for Protein Function and Design, University Chemical Laboratory, Lensfield Road, Cambridge CB2 1EW, U.K.
Received June 30, 1989; Revised Manuscript Received September 8, 1989

ABSTRACT: Pre-steady-state kinetic analyses on the formation of tyrosyl adenylate from tyrosine and each of the four diastereomers of α- and β-phosphorothioate adenosine triphosphates [ATPαS and ATPβS; Eckstein, F., & Goody, R. (1976) *Biochemistry 15*, 1685–1691; Yee, D., Armstrong, V. W., & Eckstein, F. (1979) *Biochemistry 18*, 4116–4123] were performed in the presence of Mg^{2+}, Co^{2+}, and Cd^{2+} as the divalent metal ion cofactor. A modest preference of 5.5-fold in k_3/K_A' (where k_3 is the rate constant for tyrosyl adenylate formation and K_A' is the dissociation constant for ATP, or phosphorothioate ATP, from the E·Tyr·metal·ATP complex) for the S_P ATPαS diastereomer and the absence of an inversion of preference when the metal ion is changed suggest that there is a stereospecific enzyme–α-phosphate interaction and that there is no direct metal ion interaction with the α-phosphate. The extent of reaction of the ATPαS diastereomers (30–50%) implies that these analogues are more susceptible to the hydrolytic site reaction previously reported for this enzyme [Wells, T. N. C., & Fersht, A. R. (1986) *Biochemistry 25*, 1881–1886]. The strong preference in k_3/K_A' for the R_P ATPβS diastereomer (16-fold for Mg^{2+} and 50-fold for Co^{2+}) is indicative of a stereospecific interaction with the pro $S_{P\beta}$ oxygen of ATP. The S_P ATPβS diastereomer exhibits an unusually low extent of reaction ($\sim$10% versus 70–100% for the R_P diastereomer) that does not appear to be due to the hydrolytic side reaction. This low extent of reaction appears to mask the inversion of preference in k_3 and k_3/K_A' when the metal ion is changed. The observed change in preference in K_A' (S_P/R_P for Mg^{2+} = 1.8 and for Cd^{2+} = 0.36) is consistent with metal ion binding to the β-phosphate. A model of the E·Tyr·Mg·ATP complex is proposed that involves enzyme binding to the *pro*-$R_{P\alpha}$ oxygen and Mg^{2+} chelating to the *pro*-$S_{P\beta}$ oxygen of ATP.

The tyrosyl-tRNA synthetase from *Bacillus stearothermophilus* catalyzes the aminoacylation of $tRNA^{tyr}$ [1] with tyrosine in a two-step mechanism.

$$\text{Tyr} + \text{Mg·ATP} \rightleftharpoons \text{Tyr-AMP} + \text{Mg·PP}_i \quad (1)$$

$$\text{Tyr-AMP} + \text{tRNA} \rightleftharpoons \text{Tyr-tRNA} + \text{AMP} \quad (2)$$

In the first step (eq 1), termed "tyrosine activation", the tyrosyl adenylate formed is tightly bound by the enzyme. In the second step (eq 2), transfer of tyrosine from the tyrosyl adenylate to the tRNA occurs. In the absence of tRNA, the enzyme tyrosyl adenylate complex is stable and provides an accurate means of active-site titration (Fersht et al., 1975). A number of three-dimensional X-ray crystal structures of wild-type and mutant enzymes and of the E·Tyr and the E·Tyr-AMP complexes have been solved (Monteilhet et al., 1984; Brown et al., 1987; Brown, 1988; Fothergill, 1988). However, the magnesium ion cofactor is not seen in any of these structures. Site-directed mutagenesis experiments on the synthetase have revealed many protein residues that are involved in specific binding interactions with the substrates, transition states, and products of the reaction [reviewed in Fersht (1987)], but the exact role of the metal ion has remained obscure.

Phosphorothioate analogues of ATP (Figure 1) have been widely used for the determination of the configuration of the metal–ATP substrate complex in enzymatic reactions by measuring kinetic parameters of the enzymatic reaction with the diastereomers of ATPαS and ATPβS in the presence of various metal ions (Eckstein, 1985). The basis of this method is that Mg^{2+} preferentially coordinates to oxygen, Co^{2+} exhibits little selectivity, and Cd^{2+} preferentially coordinates to sulfur (Pecoraro et al., 1984). Thus, if the metal ion is coordinated to either the α or β phosphate during the reaction, then a change in stereoselectivity for the two diastereomers of ATPαS

† This work supported by the MRC of the U.K. (A.R.F. and R.J.L.) and an NIH Postdoctoral Fellowship (GM12401, G.A.G.).
‖ Present address: College of Pharmacy, The University of Michigan, 428 Church St., Ann Arbor, MI 48109-1065.
‡ Department of Chemistry, Imperial College of Science and Technology, London SW7 2AZ, U.K.
§ Max-Planck Institut für Experimentelle Medizin, Abteilung Chemie, Hermann-Tein-Str. 3, D-3400 Göttingen, BRD.

[1] Abbreviations: tRNA, transfer ribonucleic acid; ATP, adenosine 5′-triphosphate; S_P, *S* stereoisomer at phosphorus; R_P, *R* stereoisomer at phosphorus.

0006-2960/90/0429-1643$02.50/0

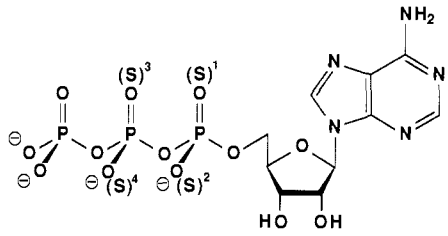

FIGURE 1: Phosphorothioate ATP analogues (1 = R_P ATPαS isomer; 2 = S_P ATPαS isomer; 3 = S_P ATPβS isomer; 4 = R_P ATPβS isomer).

or ATPβS is to be expected (Cohn, 1982).

In this paper we report pre-steady-state kinetic experiments on aminoacyl adenylate formation with the tyrosyl-tRNA synthetase using α- and β-phosphorothioate ATP analogues with Mg^{2+}, Co^{2+}, and Cd^{2+} as the divalent metal cation. These experiments establish both the catalytic rate constants and the binding constants for each of the phosphorothioate ATP analogues with each of the metal ions. Conclusions about the binding geometry of the metal ion in the E·Tyr·Mg·ATP complex are made from these data.

Materials and Methods

The diastereomers of ATPαS and ATPβS were prepared as described previously (Eckstein & Goody, 1976; Yee et al., 1979). The ATP analogues were characterized by ^{31}P NMR spectroscopy and reverse-phase HPLC as previously described for the diastereomers of ATPαS (Ludwig & Eckstein, 1989). For the HPLC analysis of the diastereomers of ATPβS, the same system was used except that the triethylammonium bicarbonate buffer contained 20 mM $MgCl_2$ and the acetonitrile concentration was linearly increased from 0 to 4.5% over 15 min (Marquetant & Goody, 1983). This led to a partial resolution of the two diastereomers with retention times for the S_P isomer of 4.83 min and for the R_P isomer of 5.18 min. The ^{31}P NMR spectra of the diastereomers of ATPβS were identical with those reported earlier (Sheu & Frey, 1977).

The tyrosyl-tRNA synthetase from *B. stearothermophilus* was expressed in *Escherichia coli* TG2 hosts from M13mp9 phage constructed as described previously (Carter et al., 1984) and purified to electrophoretic homogeneity according to the method of Wells and Fersht (1986). Uniformly labeled [^{14}C]tyrosine (486 mCi/mmol) was purchased from Amersham. Inorganic pyrophosphatase, Trizma base, Bis-tris, and chelating resin were purchased from Sigma. Nitrocellulose disks (type 11306) were obtained from Sartorius. Magnesium and cobalt were used as their chloride salts. Cadmium was present as its acetate salt.

Kinetics. Assay mixtures contained the following: 144 mM Tris buffer (pH 7.78), 1 unit/100 μL inorganic pyrophosphatase, 19 μM [U-^{14}C]tyrosine, 0.8 μM tyrosyl-tRNA synthetase, and 0.05–20 mM phosphorothioate ATP. Additionally, in their respective reactions, magnesium and cobalt concentrations were maintained at a 5 mM excess over the phosphorothioate ATP concentration. Due to apparent substrate inhibition in the cadmium reactions at concentrations ≥5 mM, the cadmium concentration was maintained at a 2 mM excess over that of the phosphorothioate ATPs. A small amount (~10 mg) of chelating resin was added to buffer/tyrosine and enzyme stocks to remove any traces of divalent metal that might interfere in the assays. The chelating resin was removed by centrifuging and decanting stock solutions prior to use. Trial assays performed in the presence and absence of magnesium ion were used to detect the presence of contaminating metal ions. The phosphorothioate ATP solutions were either treated with chelating resin as above or extracted with a 1% solution of 8-hydroxyquinoline in chloroform to remove trace metal ions. It should be noted that the chelating resin does adsorb a small amount of tyrosine and ATP. Tyrosine and ATP analogue concentrations were determined spectrophotometrically after metal ion removal treatment.

Assays were performed at 25 °C by filtering 20-μL aliquots taken at various incubation times up to 40 min through nitrocellulose filters. The filters had been prewashed with 144 mM Tris buffer (pH 7.78) saturated with tyrosine to reduce background radioactivity due to adsorption of [U-^{14}C]tyrosine to the filters. Filters were dried and counted in OptiPhase HiSafe II (LKB) liquid scintillant for 10 min each. Tyrosyl adenylation rates (k_{obs}) were calculated by using Enzfitter (Elsevier-Biosoft) to perform a nonlinear fit of the data to a first-order rate equation. Corrected rate constants (k_3') were then fit (nonlinear) to Michaelis–Menten kinetics. Standard errors were calculated by using the method of Cleland (1967).

Assays with Cd·ATPβS at pH 6.0 were performed exactly as described above with the exception that the buffer was 100 mM Bis-tris (pH 6.0).

Results

Initial steady-state tRNA charging experiments (data not shown) determined that both Co^{2+} and Cd^{2+} are able to substitute for Mg^{2+} in the tyrosyl-tRNA synthetase reaction. At concentrations greater than 5 mM, substrate inhibition was observed with Cd·ATP. This inhibition is presumably due to Cd^{2+} interaction with protein thiol groups. For all of the subsequent studies Mg^{2+} and Co^{2+} were present in 5 mM excess and Cd^{2+} was present in 2 mM excess.

Steady-state tRNA charging experiments (data not shown) performed with the phosphorothioate ATP analogues revealed that the analogues reacted much more slowly than ATP in the tyrosyl-tRNA synthetase reaction. The rates were sufficiently low (<0.01 versus 38 s^{-1} for ATP) that pre-steady-state kinetic analyses on aminoacyl adenylate formation could be performed by a slight modification of the active-site titration assay described previously (Fersht et al., 1975). These pre-steady-state analyses yield both k_3, the unimolecular rate constant for tyrosyl adenylate formation from the E·Tyr·M·ATPS complex (M represents the divalent metal ion), and K_A', the true dissociation constant of the M·ATPS from the E·Tyr·M·ATPS complex.

$$\text{E·Tyr} + \text{M·ATP} \overset{K_A'}{\rightleftharpoons} \text{E·Tyr·M·ATP} \underset{k_{-3}}{\overset{k_3}{\rightleftharpoons}} \text{E·Tyr-AMP} + \text{M·PP}_i \qquad (3)$$

$$\text{E·Tyr·M·ATP} \xrightarrow{k_{hyd}} \text{E·Tyr·AMP}$$

Kinetics. Formation of tyrosyl adenylate is followed by a hydrolytic side reaction (eq 3; Wells et al., 1986). In this side reaction, enzyme-bound tyrosyl adenylate is hydrolyzed to tyrosine and AMP, which then dissociate from the enzyme. [This reaction actually occurs via two pathways, the first being hydrolysis on the enzyme and the second being via dissociation of the Tyr-AMP and subsequent hydrolysis in solution (see Discussion). For the purposes of correcting the observed formation rates, the hydrolysis reaction may be treated as occurring via a single step.] Because of hydrolysis, the E·Tyr-AMP complex does not build up to 100%, but reaches a steady-state plateau. Consequently, the observed rate constant for formation of tyrosyl adenylate (k_{obs}) is larger than the rate constant k_3. Solution of the first-order rate equation for the observed rate (k_{obs}) and the amount of E·Tyr-AMP complex formed (amplitude) gives

$$k_{obs} = k_3' + k_{hyd} \quad (4)$$

where

$$k_3' = k_3[ATP]/(K_A' + [ATP]) \quad (5)$$

$$\text{amplitude} = k_3'[E_0]/(k_3' + k_{hyd}) \quad (6)$$

The amplitude and k_{obs} are calculated from the first-order fit of the data. Dividing the amplitude by the enzyme concentration, determined by the active-site titration assay, gives the extent of reaction:

$$\text{extent of reaction} = k_3'/(k_3' + k_{hyd}) \quad (7)$$

In practice, the extent of reaction is calculated as the ratio of $[E\cdot Tyr\text{-}AMP]_{observed}$, from the first-order analysis, to $[E\cdot Tyr\text{-}AMP]_{expected}$, calculated from the enzyme concentration. Therefore, k_3' is given by k_{obs} times the extent of reaction:

$$k_3' = k_{obs} \times \text{extent of reaction} \quad (8)$$

$$k_3' = k_{obs}([E\cdot Tyr\text{-}AMP]_{observed}/[E\cdot Tyr\text{-}AMP]_{expected}) \quad (9)$$

Alternatively, one can use initial rates to analyze the data. In this case, k_3' is obtained directly from the initial velocity v_0:

$$k_3' = v_0/[E_0] \quad (10)$$

Corrected rates are then plotted against ATP analogue concentration and nonlinearly fit to Michaelis–Menten kinetics, yielding k_3 and K_A'.

ATPαS. Table I lists the pre-steady-state kinetic parameters for the ATPαS diastereomers with each of the three metal ions. Only k_3/K_A' values for the cadmium reactions are reported because the K_A's for the Cd·ATPαS analogues were, in both cases, greater than 5 mM. Only the initial, linear portion of the Michaelis–Menten curve was determined, yielding k_3/K_A' values only. These values can be compared to those for Mg·ATP, where $k_3 = 38\ s^{-1}$, $K_A' = 4.7$ mM, and $k_3/K_A' = 8085\ s^{-1}\ M^{-1}$.

The relative kinetic parameters, calculated as a simple ratio of the value for the S_P isomer over that for the R_P isomer, are listed in Table II. Within experimental error, there is no isomeric preference with either Co^{2+} or Cd^{2+}. For Mg^{2+}, there is a 5-fold preference in k_3/K_A' for the S_P isomer. This preference appears to come from K_A', since the preference in k_3 is small and may be negligible, within experimental error.

ATPβS. The pre-steady-state kinetic parameters for the ATPβS stereoisomers are listed in Table III. The relative kinetic parameters are listed in Table IV. There is a large preference for the R_P isomer in k_3, K_A', and k_3/K_A' for both Mg^{2+} and Co^{2+}. The preference in k_3 and k_3/K_A' for Cd^{2+} is also for the R_P isomer, but is less strong in k_3/K_A'. The preference in K_A' for Cd^{2+} is reversed, but may be negligible within experimental error.

Extent of Reaction. The extents of reaction for each of the phosphorothioate ATP analogues at 1 mM concentration with each of the three metal ions are given in Table V. The ATPαS analogues give between 30 and 50% reaction. The R_P ATPβS isomer gives between 74 and 100% reaction. However, the S_P ATPβS isomer only gives between 7 and 17% reaction. This very low level of tyrosyl adenylate formation with the S_P ATPβS isomer (extremely low for the Cd^{2+} reaction, ~7%) may mask any inversion of preference that might have been observed when the metal was changed from Mg^{2+} to Cd^{2+}. To determine if the low extent of reaction of the S_P ATPβS isomer is due to the hydrolytic side reaction, tyrosyl adenylate formation assays for the ATPβS analogues with Cd^{2+} were performed at pH 6.0 (data not shown). For the R_P isomer, the K_A' was 0.24 mM and k_3 was $0.001\ s^{-1}$ (50% less than at pH 7.78). Substrate inhibition was observed at R_P isomer concentrations greater than 1 mM. The S_P isomer showed essentially no reaction at concentrations from 0.1 to 2.0 mM.

Table I: Pre-Steady-State Kinetic Parameters for ATPαS S_P and R_P Isomers[a]

isomer	metal ion	k_3 ($\times 10^3\ s^{-1}$)	K_A' (mM)	k_3/K_A'' ($s^{-1}\ M^{-1}$)
S_P	Mg^{2+}	1.8 (±0.4)[b]	0.11 (±0.05)	16
S_P	Co^{2+}	4.2 (±1.6)	4.3 (±2)	0.98
S_P	Cd^{2+}	[c]	[c]	1.3
R_P	Mg^{2+}	2.4 (±0.6)	0.82 (±0.37)	2.9
R_P	Co^{2+}	3.7 (±0.3)	4.3 (±0.5)	0.87
R_P	Cd^{2+}	[c]	[c]	1.05

[a] Reaction conditions: 25 °C, 144 mM Tris (pH 7.78), 19 μM [U-^{14}C]tyrosine, 1 unit/100 μL inorganic pyrophosphatase, 0.8 μM tyrosyl-tRNA synthetase, and 0.05–20 mM ATPαS. Mg^{2+} and Co^{2+} were present in 5 mM excess, and Cd^{2+} was present in 2 mM excess. [b] Numbers in parentheses are standard errors. [c] Not measurable due to high K_A' and inhibition by cadmium at concentrations ≥5 mM.

Table II: Relative Kinetic Parameters for ATPαS Isomers S_P/R_P

metal ion	$k_3(S_P)/k_3(R_P)$	$K_A'(S_P)/K_A'(R_P)$	$k_3/K_A'(S_P)/k_3/K_A'(R_P)$
Mg^{2+}	0.75	0.14	5.5
Co^{2+}	1.1	1.0	1.1
Cd^{2+}	[a]	[a]	1.2

[a] Not measurable due to high K_A' and inhibition by cadmium at concentrations ≥5 mM.

Table III: Pre-Steady-State Kinetic Parameters for ATPβS S_P and R_P Isomers[a]

isomer	metal ion	k_3 ($\times 10^3\ s^{-1}$)	K_A' (mM)	k_3/K_A'' ($s^{-1}\ M^{-1}$)
S_P	Mg^{2+}	1.6 (±0.2)	2.8 (±0.7)	0.60
S_P	Co^{2+}	2.4 (±0.9)	12.8 (±6.0)	0.19
S_P	Cd^{2+}	0.13 (±0.1)	0.50 (±0.1)	0.26
R_P	Mg^{2+}	15 (±1.6)	1.6 (±0.4)	9.4
R_P	Co^{2+}	11.0 (±1.4)	1.2 (±0.3)	9.2
R_P	Cd^{2+}	1.9 (±0.6)	1.4 (±0.8)	1.4

[a] Reaction conditions identical with those for Table I.

Table IV: Relative Kinetic Parameters for ATPβS Isomers S_P/R_P

metal ion	$k_3(S_P)/k_3(R_P)$	$K_A'(S_P)/K_A'(R_P)$	$k_3/K_A'(S_P)/k_3/K_A'(R_P)$
Mg^{2+}	0.11	1.8	0.061
Co^{2+}	0.22	11	0.021
Cd^{2+}	0.07	0.36	0.19

Table V: Extents of Reaction for 1 mM ATPS[a]

	ATPαS (%)		ATPβS (%)	
metal ion	R_P	S_P	R_P	S_P
Mg^{2+}	51	36	113	17
Co^{2+}	32	32	84	10
Cd^{2+}	38	44	74	7

[a] $([E\cdot Tyr\text{-}AMP]_{observed}/[E\cdot Tyr\text{-}AMP]_{expected}) \times 100$.

Discussion

The first use of a phosphorothioate ATP analogue (ATPαS) for the elucidation of the mechanism of an aminoacyl-tRNA synthetase was reported by Von der Haar et al. (1977) in their study of the phenylalanyl-tRNA synthetase from yeast. Connolly et al. (1980) extended that study and used phosphorothioate ATP analogues to deduce the absolute geometry of the metal ion binding to ATP for that synthetase.

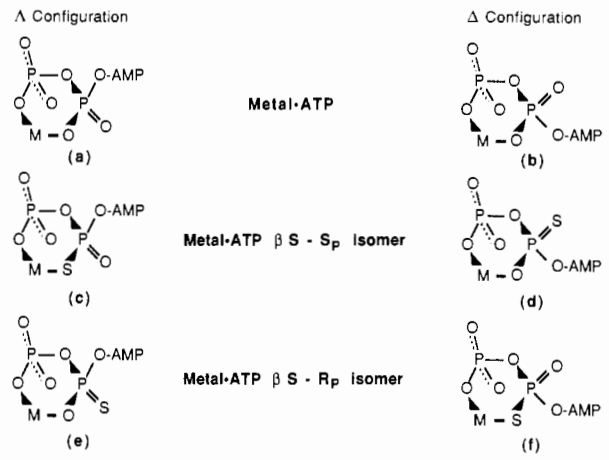

FIGURE 2: Absolute configurations of the β,γ-bidentate metal ion (M) complexes of ATP and ATPβS [adapted from Connolly et al. (1980)].

Steady-state kinetic analyses of pyrophosphate exchange (where [^{32}P]pyrophosphate is exchanged into ATP in the absence of tRNA) and aminoacyl-tRNA formation (tRNA charging) with each of the phosphorothioate ATP analogues with Mg^{2+} and Co^{2+} revealed the stereoisomeric preferences (of V_{max}/K_m) for these metal ions. The α isomers were inactive with Cd^{2+}, and for the β isomers only a ratio of tRNA charging rates at 1 mM ATPβS and 0.1 mM Cd^{2+} was determined. From these data, the investigators deduced that the metal ion binds to ATP in a β,γ-bidentate complex with the Λ configuration (Figure 2). These authors observed an unusual β to γ interchange reaction previously reported by Rossomando et al. (1979) in which the phosphorothioate is transferred from the β position to the γ position. However, the stereoisomeric preference for the interchange reaction determined by Connolly et al. (1980) was identical with that for pyrophosphate exchange and tRNA charging. They also found that while there was no difference in activity of the ATPαS stereoisomers when the metal ion was changed, only the S_P isomer was a substrate. This led the authors to conclude that there is a specific interaction between the protein and the α-phosphate of the ATP that requires an oxygen atom in the *pro*-$R_{P\beta}$ position. Smith and Cohn (1982) performed a study with the methionyl-tRNA synthetase from *E. coli*. In this study, they used Zn^{2+} as the sulfur-preferring metal ion. The R_P ATPαS isomer was inactive with either metal ion in either pyrophosphate exchange or tRNA charging. The S_P ATPαS isomer was active only with Mg^{2+}. The ATPβS analogues exhibited a 21 000-fold preference in V_{max} for the S_P isomer in the presence of Mg^{2+} and a 20-fold preference for the R_P isomer with Zn^{2+}. A ratio of pyrophosphate exchange rates at 2 mM methionine, 1 mM [^{32}P]pyrophosphate, and 1 mM ATPβS exhibited essentially the same preferences. These authors also concluded that the metal ion chelates in a β,γ-bidentate complex, however, with the Δ configuration. In a study of the tryptophanyl-tRNA synthetase from yeast, Piel et al. (1983) reported pyrophosphate exchange kinetics on phosphorothioate ATP analogues. They determined that Mg^{2+} interacts only with the S_P ATPαS and the S_P ATPβS isomers and that Zn^{2+} only interacts with the R_P ATPβS isomer. They concluded that, like the methionyl-tRNA synthetase, the metal ion coordinates in a β,γ-bidentate complex with the Δ configuration.

ATPαS. Unlike the studies reported by Connolly et al. (1980) and Smith and Cohn (1982), both ATPαS isomers are substrates for the tyrosyl-tRNA synthetase. However, in their study of the phenylalanyl-tRNA synthetase from *E. coli*., Pimmer et al. (1976) reported that all five phosphorothioate ATP analogues (they also tested ATPγS) are substrates in the reaction with Mg^{2+} and that their V_{max} values are approximately 20% of that for ATP. They noted that there is only a very small discrimination between the stereoisomeric pairs. Within experimental error, we find that the reactions with Co^{2+} and Cd^{2+} show no significant preference for either α isomer. In contrast, the reaction with Mg^{2+} exhibits a 7.3-fold binding preference for the S_P isomer. The ATPαS analogues are bound much more tightly (5–40 times) in their complex with Mg^{2+} than with the other metal ions. In this tight complex, the Mg^{2+} most probably tethers the β- and γ-phosphates to the enzyme, forcing the α-phosphate into a position where an enzymatic residue stereospecifically interacts with one of the oxygens, resulting in the observed diastereomeric preference. The looser complexes formed with Co^{2+} and Cd^{2+} show no discriminatory interaction. The lack of any inversion of preference upon changing the metal ion suggests that there is no direct interaction between the metal ion and the α-phosphate, consistent with the argument that the observed diastereomeric preference in binding in the presence of Mg^{2+} is due to tighter binding of the β- and γ-phosphates. The absence of preference with Co^{2+} and Cd^{2+} and the small preference with Mg^{2+} imply that the interaction between the protein and the α-phosphate is weakly stereospecific and is involved only in binding, not in catalysis.

The presence of sulfur on the α-phosphate slows down the rate of tyrosyl adenylate formation by some 5 orders of magnitude ($\sim 10^{-3}$ versus 38 s^{-1} for Mg·ATP). At present, there is no nonenzymatic reaction reported from which one could deduce a value for the elemental P=O/P=S effect in this reaction. The only model reaction available is the base-catalyzed hydrolysis of triethyl phosphate and phosphorothioate (Ketelaar et al., 1952). The rate of hydrolysis of the latter is reduced by a factor of 30. There are, however, a few enzyme-catalyzed reactions for which the rates of nucleophilic substitution at phosphates and phosphorothioates have been compared by pre-steady-state kinetics. This effect is about 3–7-fold in the large fragment of *E. coli* DNA polymerase (Klenow) catalyzed polymerization step of dATP versus dATPαS (Kuchta et al., 1987). A much larger effect of approximately 700-fold is seen for the myosin-catalyzed hydrolysis of ATP and ATPγS (Bagshaw et al., 1972). An even larger value of 2500-fold has been observed for the GTP and GTPγS hydrolysis catalyzed by the EF Tu factor (Thompson & Karim, 1982). Thus, although at present no definitive value can be put on the elemental effect, it probably is not more than 2 orders of magnitude. The larger effects seen in the enzyme-catalyzed reactions might well be due to an imperfect alignment of the functional groupos on the enzyme with the substrate analogue. There is a crucial difference between enzymatic and nonenzymatic reactions, and that is that the enzymatic groups that are involved in solvating the transition state have a fixed geometry. When water solvates the transition state for the same reaction, the water is capable of adjusting its position to accommodate the different geometries of the transition states for the phosphate versus phosphorothioate reactions. The tyrosyl-tRNA synthetase uses a mobile loop that binds to the triphosphate moiety of ATP to stabilize the transition state for tyrosyl adenylate formation. Mutation of either Lys 230 or Lys 233 to alanine reduces k_3 by 2–3 orders of magnitude (Fersht et al., 1988). Negative interactions between the phosphorothioate ATP analogues and the mobile loop of the enzyme may account for the additional 3 orders of magntidue in rate reduction over that due to the elemental effect. Aminoacyl-tRNA synthetases vary greatly

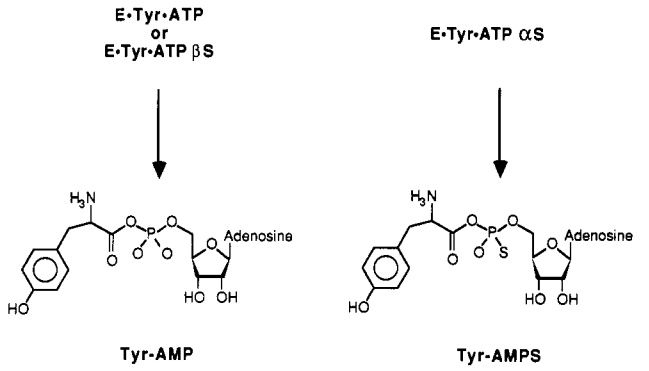

FIGURE 3: Tyrosyl adenylate formed from ATP and ATPβS and from ATPαS.

in size and structure (Schimmel & Söll, 1979), and not all may have this mobile loop.

The extent of reaction for the ATPαS analogues (30–50%) implies that the rate of hydrolysis (k_{hyd}) is on the same order of magnitude as the rate of tyrosyl adenylate formation (k_3). One possible explanation is that the hydrolysis rate on the enzyme for Tyr-AMPS (Figure 3) may be increased by approximately 2 orders of magnitude over that for Tyr-AMP (k_{he} = 5.14 × 10^{-5} s^{-1}; Wells et al., 1986). This increase in hydrolysis rate for the tyrosyl AMPS would be inconsistent with the expected decrease in rate due to the elemental effect if the hydrolysis reaction occurred via a nucleophilic substitution at phosphorus. However, if water (or hydroxide) attacks the carbonyl carbon of this mixed anhydride and adenosine 5′-phosphorothioate (AMPS) ion is the leaving group, then an increase in rate is to be expected because of the lower pK_a of this anion in comparison to that of AMP (Jaffe & Cohn, 1978). A second, and perhaps more likely, explanation for the observed extent of reaction for the ATPαS analogues is that the Tyr-AMPS is dissociating from the enzyme and hydrolyzing in solution. Wells et al. (1986) determined that the hydrolysis of Tyr-AMP occurs via two pathways.

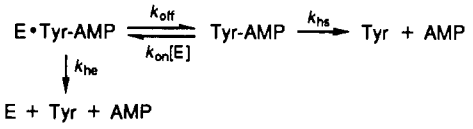

In the first pathway, hydrolysis occurs on the enzyme with a rate constant (k_{he}), for wild-type enzyme, of 5.14 × 10^{-5} s^{-1}. The second pathway involves rate-determining dissociation of Tyr-AMP from the enzyme (k_{off}) = 6.7 × 10^{-4} s^{-1}) and subsequent hydrolysis in solution (k_{hs} = 7.6 × 10^{-3} s^{-1}). Clearly, if Tyr-AMPS dissociates 5–10 times faster than Tyr-AMP, then the effective hydrolysis rate becomes approximately equal to the Tyr-AMPS formation rate (k_3).

ATPβS. The R_P ATPβS isomer reacts approximately 5-fold faster (k_3 is 5-fold larger) than either of the ATPαS analogues. This most probably is a result of transferring the sulfur atom to the β-phosphate, away from the center of the reaction at the α-phosphate. The high extent of reaction of the β R_P isomer (70–100%) is consistent with the argument that the lower extents of reaction observed for the α analogues are due to the presence of the sulfur atom in the tyrosyl adenylate (Figure 3). The sulfur atom of the R_P ATPβS isomer would end up in the pyrophosphate moiety and would not be expected to influence the hydrolysis or binding of the tyrosyl adenylate. In this case, the hydrolysis rate may not be much higher than for the reaction with ATP. The observed extent of reaction is probably due to the lower of k_3 by 4 orders of magnitude from that of ATP, making the hydrolytic side reaction significant for the reactions with Co^{2+} and Cd^{2+}, where k_3 is even lower than for the reaction with Mg^{2+}.

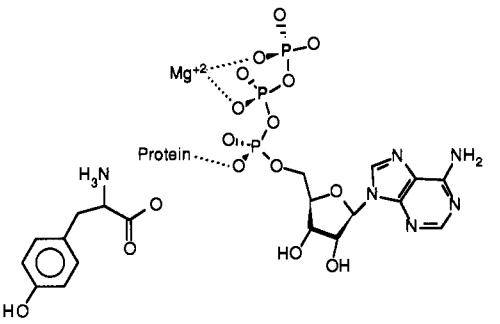

FIGURE 4: Deduced interactions within the E·Tyr·Mg·ATP complex.

The S_P ATPβS isomer appears to be an extremely poor substrate. The very low extent of reaction (~10%) appears not to be due to the hydrolytic side reaction. The lack of reaction at pH 6.0, where k_{hyd} is slowed considerably, and the high extent of reaction for the R_P ATPβS isomer are inconsistent with a high hydrolysis rate. (The k_{hyd} would have to be 9 times larger than k_3 to result in a 10% extent of reaction.) The inactivity of the S_P isomer masks the attempt to detect an inversion of isomeric preference when the metal ion is changed. There does appear to be an inversion of preference in K_A' upon going from Mg^{2+} to Cd^{2+}, but, within experimental error, this may not be significant.

Conclusions

Figure 4 sketches the interactions of the E·Tyr·Mg·ATP complex deduced from the data in this study which may be added to those deduced previously (Fersht, 1987). The 7.3-fold preference in binding of the Mg·ATPαS S_P isomer indicates that there is a protein interaction with the *pro-*$R_{P\alpha}$ oxygen of ATP. The absence of an inversion of preference when the metal ion is changed suggests that there is no direct interaction between the Mg^{2+} and the α-phosphate of ATP. The inactivity of the ATPβS S_P isomer makes it difficult to draw any firm conclusions. However, the reversal of K_A' preference for β isomer implies that there is metal ion coordination to the β-phosphate of ATP. The observed preference for the R_P isomer by Mg^{2+} suggests that the metal ion binds stereospecifically to the *pro-*$S_{P\beta}$ oxygen of ATP in the Λ configuration. This configuration is the same as that found by Connolly et al. (1980) and opposite to that found by Rossomando et al. (1979) and Piel et al. (1983).

Registry No. S_P-ATPαS, 58976-48-0; R_P-ATPαS, 58976-49-1; S_P-ATPβS, 59261-36-8; R_P-ATPβS, 59261-35-7; Mg, 7439-95-4; Co, 7440-48-4; Cd, 7440-43-9; tyrosyl-tRNA synthetase, 9023-45-4.

References

Bagshaw, C. R., Eccleston, J. F., Trentham, D. R., Yates, D. W., & Goody, R. S. (1972) *Cold Spring Harbor Symp. Quant. Biol. 37*, 127–136.

Brown, K. (1988) Ph.D. Dissertation, University of London.

Brown, K., Brick, P., & Blow, D. M. (1987) *Nature 326*, 416–418.

Carter, P., Winter, G., Wilkinson, A. J., & Fersht, A. R. (1984) *Cell (Cambridge, Mass.) 38*, 835–840.

Cleland, W. W. (1967) *Adv. Enzymol. Relat. Areas Mol. Biol. 29*, 1–32.

Cohn, M. (1982) *Acc. Chem. Res. 15*, 326–332.

Connolly, B. A., Von der Haar, F., & Eckstein, F. (1980) *J. Biol. Chem. 255*, 11301–11307.

Eckstein, F. (1985) *Annu. Rev. Biochem. 54*, 367–402.

Eckstein, F., & Goody, R. S. (1976) *Biochemistry 15*, 1685–1691.

Fersht, A. R. (1987) *Biochemistry 26*, 8031-8037.
Fersht, A. R., Ashford, J., Bruton, C., Jakes, R., Koch, G., & Hartley, B. (1975) *Biochemistry 14*, 1-13.
Fersht, A. R., Knill-Jones, J. W., Bedouelle, H., & Winter, G. (1988) *Biochemistry 27*, 1581-1587.
Fothergill, M. D. (1988) Ph.D. Dissertation, University of London.
Jaffe, E. K., & Cohn, M. (1978) *Biochemistry 17*, 652-657.
Ketelaar, J. A. A., Gersmann, H. R., & Koopmans, K. (1952) *Recl. Trav. Chim. Pays-Bas 71*, 1253.
Kuchta, R. D., Mizrahi, V., Benkovic, P. A., Johnson, K. A., & Benkovic, S. J. (1987) *Biochemistry 26*, 8410-8417.
Ludwig, J., & Eckstein, F. (1989) *J. Org. Chem. 54*, 631-635.
Marquetant, R., & Goody, R. S. (1983) *J. Chromatogr. 280*, 386-389.
Monteilhet, C., Blow, D. M., & Brick, P. (1984) *J. Mol. Biol. 173*, 477-485.
Mulvey, R. S., & Fersht, A. R. (1977) *Biochemistry 16*, 4005-4013.
Pecoraro, V. L., Hermes, J. D., & Cleland, W. W. (1984) *Biochemistry 23*, 5262-5271.
Piel, N., Freist, W., & Cramer, F. (1983) *Bioorg. Chem. 12*, 18-33.
Pimmer, J., Holler, E., & Eckstein, F. (1976) *Eur. J. Biochem. 67*, 171-176.
Rossomando, E. F., Smith, L. T., & Cohn, M. (1979) *Biochemistry 18*, 5670-5676.
Schimmel, P., & Söll, D. (1979) *Annu. Rev. Biochem. 48*, 601-648.
Sheu, K.-F. R., & Frey, P. A. (1977) *J. Biol. Chem. 252*, 4445-4448.
Smith, L. T., & Cohn, M. (1982) *Biochemistry 21*, 1530-1534.
Thompson, R. C., & Karim, A. M. (1982) *Proc. Natl. Acad. Sci. U.S.A. 79*, 4922-4926.
Von der Haar, F., Cramer, F., Eckstein, F., & Stahl, K. W. (1977) *Eur. J. Biochem. 76*, 263-267.
Wells, T. N. C., & Fersht, A. R. (1986) *Biochemistry 25*, 1881-1886.
Wells, T. N. C., Ho, C. K., & Fersht, A. R. (1986) *Biochemistry 25*, 6603-6608.
Yee, D., Armstrong, V. W., & Eckstein, F. (1979) *Biochemistry 18*, 4116-4123.

12-[(5-Iodo-4-azido-2-hydroxybenzoyl)amino]dodecanoic Acid: Biological Recognition by Cholesterol Esterase and Acyl-CoA:Cholesterol *O*-Acyltransferase†

Paula M. Kinnunen, Fredric H. Klopf, Carol A. Bastiani, Claire M. Gelfman, and Louis G. Lange*
Department of Medicine, Division of Cardiology, Jewish Hospital of St. Louis at the Washington University Medical Center, St. Louis, Missouri 63110

Received August 1, 1989; Revised Manuscript Received October 9, 1989

ABSTRACT: Potential probes of protein cholesterol and fatty acid binding sites, namely, 12-[(5-iodo-4-azido-2-hydroxybenzoyl)amino]dodecanoate (IFA) and its coenzyme A (IFA:CoA) and cholesteryl (IFA:CEA) esters, were synthesized. These radioactive, photoreactive lipid analogues were recognized as substrates and inhibitors of acyl-CoA:cholesterol *O*-acyltransferase (ACAT) and cholesterol esterase, neutral lipid binding enzymes which are key elements in the regulation of cellular cholesterol metabolism. In the dark, IFA reversibly inhibited cholesteryl [^{14}C]oleate hydrolysis by purified bovine pancreatic cholesterol esterase with an apparent K_i of 150 μM. Cholesterol esterase inhibition by IFA became irreversible after photolysis with UV light and oleic acid (1 mM) provided 50% protection against inactivation. Incubation of homogeneous bovine pancreatic cholesterol esterase with IFA:CEA resulted in its hydrolysis to IFA and cholesterol, indicating recognition of IFA:CEA as a substrate by cholesterol esterase. The coenzyme A ester, IFA:CoA, was a reversible inhibitor of microsomal ACAT activity under dark conditions (apparent K_i = 20 μM), and photolysis resulted in irreversible inhibition of enzyme activity with 87% efficiency. IFA:CoA was also recognized as a substrate by both liver and aortic microsomal ACATs, with resultant synthesis of ^{125}IFA:CEA. IFA and its derivatives, IFA:CEA and IFA:CoA, are thus inhibitors and substrates for cholesterol esterase and ACAT. Biological recognition of these photoaffinity lipid analogues will facilitate the identification and structural analysis of hitherto uncharacterized protein lipid binding sites.

Photoaffinity labeling using photoreactive lipid analogues has been of unique value in the structural study of hydrophobic proteins in their native states associated with the lipid bilayer. Lipid-soluble ligands have been used successfully for the identification and characterization of integral membrane proteins and receptors, many of which are easily denatured upon separation from cell membranes. For example, photoreactive phospholipid analogues incorporated into the surrounding membrane have been used to identify the transmembrane domains of glycophorin A and the membrane-anchoring groups of cytochrome b_5 (Ross et al., 1982; Takagaki et al., 1983).

Intracellular cholesterol metabolism involves many such highly hydrophobic, neutral lipid binding enzymes. For example, acyl-CoA:cholesterol *O*-acyltransferase (ACAT) catalyzes the intracellular synthesis of cholesteryl esters in vascular tissue, and large increases in ACAT activity are likely

† Supported in part by NIH Clinical Investigator Award 1-K08-HL01846, NHLBI FIRST Award 1R29HL42032 (P.M.K.), a grant from the Alcoholic Beverage Medical Research Foundation (P.M.K.), a Grant-in-Aid from the Missouri Affiliate, American Heart Association (P.M.K.), NIAAA R01 AA06989 (L.G.L.), and NIAAA R01 AA07656 (L.G.L.).

* Address correspondence to this author at Cardiology Research, Yalem 305, Jewish Hospital of St. Louis, 216 S. Kingshighway, St. Louis, MO 63110.

0006-2960/90/0429-1648$02.50/0